



HAL
open science

Copper intercalation at the interface of graphene and Ir(111) studied by scanning tunneling microscopy

Muriel Sicot, Yannick Fagot-Revurat, Bertrand Kierren, Guillaume Vasseur,
Daniel Malterre

► **To cite this version:**

Muriel Sicot, Yannick Fagot-Revurat, Bertrand Kierren, Guillaume Vasseur, Daniel Malterre. Copper intercalation at the interface of graphene and Ir(111) studied by scanning tunneling microscopy. Applied Physics Letters, 2014, 105 (19), pp.191603. 10.1063/1.4901165 . hal-01430734

HAL Id: hal-01430734

<https://hal.science/hal-01430734>

Submitted on 10 Jan 2017

HAL is a multi-disciplinary open access archive for the deposit and dissemination of scientific research documents, whether they are published or not. The documents may come from teaching and research institutions in France or abroad, or from public or private research centers.

L'archive ouverte pluridisciplinaire **HAL**, est destinée au dépôt et à la diffusion de documents scientifiques de niveau recherche, publiés ou non, émanant des établissements d'enseignement et de recherche français ou étrangers, des laboratoires publics ou privés.



Copper intercalation at the interface of graphene and Ir(111) studied by scanning tunneling microscopy

M. Sicot, Y. Fagot-Revurat, B. Kierren, G. Vasseur, and D. Malterre

Citation: [Applied Physics Letters](#) **105**, 191603 (2014); doi: 10.1063/1.4901165

View online: <http://dx.doi.org/10.1063/1.4901165>

View Table of Contents: <http://scitation.aip.org/content/aip/journal/apl/105/19?ver=pdfcov>

Published by the [AIP Publishing](#)

Articles you may be interested in

[Atomic-scale movement induced in nanoridges by scanning tunneling microscopy on epitaxial graphene grown on 4H-SiC\(0001\)](#)

J. Vac. Sci. Technol. B **31**, 04D101 (2013); 10.1116/1.4803137

[Hafnium intercalation between epitaxial graphene and Ir\(111\) substrate](#)

Appl. Phys. Lett. **102**, 093106 (2013); 10.1063/1.4793427

[Silicon intercalation at the interface of graphene and Ir\(111\)](#)

Appl. Phys. Lett. **100**, 083101 (2012); 10.1063/1.3687688

[Epitaxial BaTiO₃\(100\) films on Pt\(100\): A low-energy electron diffraction, scanning tunneling microscopy, and x-ray photoelectron spectroscopy study](#)

J. Chem. Phys. **135**, 104701 (2011); 10.1063/1.3633703

[Atomic structure of interface between monolayer Pd film and Ni\(111\) determined by low-energy electron diffraction and scanning tunneling microscopy](#)

J. Appl. Phys. **108**, 103521 (2010); 10.1063/1.3514156

The image shows the cover of an Applied Physics Reviews journal issue. It features a blue and orange color scheme with a molecular structure background. The text 'NEW Special Topic Sections' is prominently displayed in white. Below it, the text 'NOW ONLINE' is in yellow, followed by 'Lithium Niobate Properties and Applications: Reviews of Emerging Trends' in white. The AIP Applied Physics Reviews logo is in the bottom right corner.

NEW Special Topic Sections

NOW ONLINE
Lithium Niobate Properties and Applications:
Reviews of Emerging Trends

AIP Applied Physics Reviews

Copper intercalation at the interface of graphene and Ir(111) studied by scanning tunneling microscopy

M. Sicot,^{a)} Y. Fagot-Revurat, B. Kierren, G. Vasseur, and D. Malterre

Institut Jean Lamour, UMR 7198, CNRS Université de Lorraine, BP 70239, 54506 Vandoeuvre lès Nancy, France

(Received 25 July 2014; accepted 27 October 2014; published online 10 November 2014)

We report on the intercalation of a submonolayer of copper at 775 K underneath graphene epitaxially grown on Ir(111) studied by means of low energy electron diffraction (LEED) and scanning tunneling microscopy (STM) at 77 K. Nucleation and growth dynamics of Cu below graphene have been investigated, and, most importantly, the intercalation mechanism has been identified. First, LEED patterns reveal the pseudomorphic growth of Cu on Ir under the topmost graphene layer resulting in a large Cu in-plane lattice parameter expansion of about 6% compared to Cu(111). Second, large-scale STM topographs as a function of Cu coverage show that Cu diffusion on Ir below graphene exhibits a low energy barrier resulting in Cu accumulation at Ir step edges. As a result, the graphene sheet undergoes a strong edges reshaping. Finally, atomically-resolved STM images reveal a damaged graphene sheet at the atomic scale after metal intercalation. Point defects in graphene were shown to be carbon vacancies. According to these results, a Cu penetration path beneath graphene is proposed to occur via metal aided defect formation with no or poor self healing of the graphene sheet. This work illustrates the fact that Cu intercalation is harmful for graphene grown on Ir(111) at the atomic scale. © 2014 AIP Publishing LLC.

[<http://dx.doi.org/10.1063/1.4901165>]

Intercalation of foreign species in carbon based materials has been extensively studied for over several decades in graphite¹ and more recently in carbon nanotubes.² This process allows for the fabrication of new compounds exhibiting exceptional electronic properties such as superconductivity. The counterpart of the intercalation process in graphene has been recently shown to be also feasible between the carbon layer and its support for a wide variety of intercalant such as molecules, alkali atoms, metals or semiconducting materials. This interface engineering allows to modify the electronic properties of graphene. Other advantages can be found from the intercalant perspective since graphene can act as an efficient protective overlayer against oxidation.³ Moreover, nanostructures with novel shape and properties can be fabricated.⁴ Despite that intercalation has been established as an efficient route for tuning the coupling of graphene to its substrate, only little is known about the process itself and a better understanding is needed at the atomic scale. It would indeed allow for a better control of the final quality of the graphene, of the size and shape of the nanostructures and will give better insight into factors influencing the intercalation. One good trilayer candidate for such a study is graphene (Gr) /Cu/Ir(111) since graphene on Ir(111) is of excellent structural quality⁵ and exhibits the linear energy dispersion at Dirac point.⁶ Moreover, Cu is a particularly attracting material as it is extensively used in devices circuitry and is envisaged as a ideal substrate for mass production of graphene.⁷ Therefore, getting insight into the Gr/Cu interaction strength can be useful for future applications.

Here, we report on the investigation of the structural properties of Gr/Cu/Ir(111) trilayers. By using atomically resolved scanning tunneling microscopy (STM) images, we were able to identify the intercalation mechanism of Cu through graphene on Ir(111). Our experimental results are discussed in the light of previous works.

The experiments were carried out in an ultra high vacuum system with a base pressure of 1×10^{-10} mbar equipped with a low-temperature STM Omicron. The Ir(111) single crystal was cleaned by repeated cycles of Ar⁺ sputtering at an energy of 1.5 keV followed by a flash annealing to 1100 K. An ordered graphene monolayer (ML) was prepared by cracking on Ir(111) held at 1100 K under a propene pressure of 3×10^{-7} mbar for 5 min. Cu was evaporated from a Knudsen cell heated up at 1125 K on a sample held at room temperature at an evaporation rate of 0.1 Å/min measured with a quartz microbalance at the sample position. To intercalate, the sample was annealed after Cu deposition at 775 K for 20 to 60 min in a base pressure of 3×10^{-10} mbar. Surface coverage is given in ML where 1 ML corresponds to the surface atomic density of Ir(111). We used PtIr scissor cut tips. All microscopy measurements were performed at 77 K. The STM images were recorded at a tunneling current I_t and a bias voltage U_t where its sign corresponds to the voltage applied to the sample. All STM images presented in that work are topographs except images in Figs. 3 and 4(a), which are so-called “current” images showing small variations of the tunneling current induced by a finite time response of the feedback loop.

The Gr/Ir(111) system is known to exhibit a moiré periodicity of 2.53 nm resulting from the lattice mismatch between graphene and iridium.⁵ As a consequence, low energy electron

^{a)}muriel.sicot@univ-lorraine.fr

diffraction (LEED) patterns show satellite spots around the main spots as displayed in Fig. 1(a). After intercalation of 1 ML of Cu (for an initial thickness of 1.65 ML of Cu), satellite spots remain at the exact same positions leading to the same moiré periodicity. As a conclusion, Cu grows pseudomorphically on Ir(111) resulting in an Cu in-plane lattice expansion of about 6% compared to the Cu(111) surface. The observation of sharp satellites spots in the inset of Fig. 1(b) is a clear evidence that the structural quality of the graphene layer characterized by small moiré misorientations is preserved upon intercalation.

The STM topograph of Gr/Ir(111) in Fig. 1(c) exhibit a moiré pattern of 2.5 nm periodicity in good agreement with the LEED pattern in Fig. 1(a). Starting from this surface, 0.2 ML of Cu has been intercalated. The corresponding STM topograph is shown in Fig. 1(d). As discussed later, the tunneling

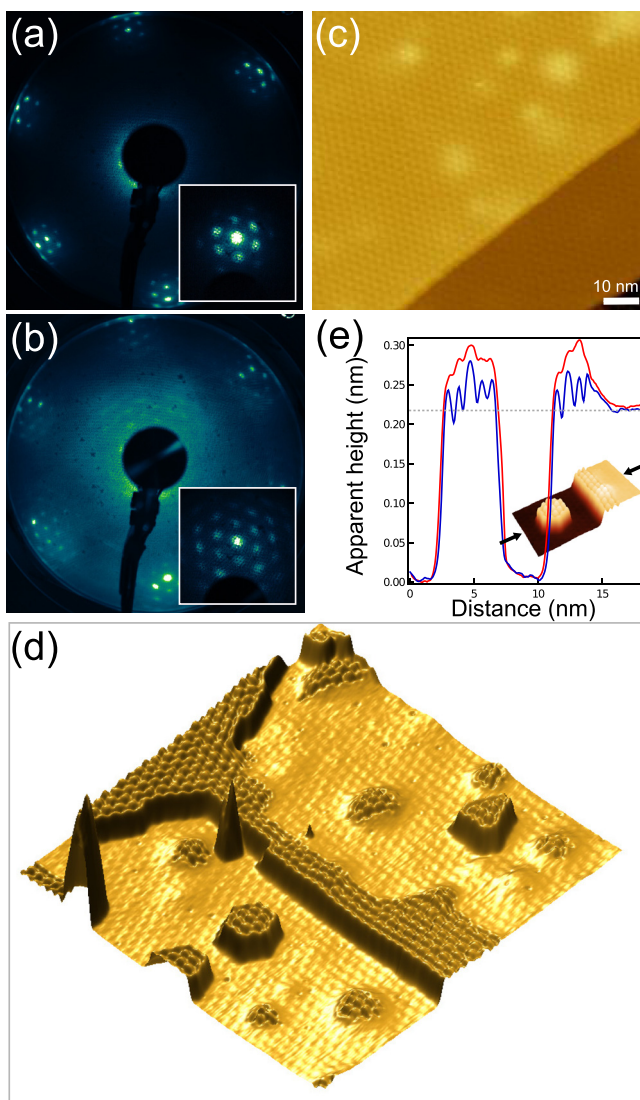


FIG. 1. LEED patterns taken at an electron energy of 77.5 eV of (a) Gr/Ir(111) and (b) Gr/1 ML Cu/Ir(111). Insets are [00] spots recorded at an electron energy of 40 eV. (c) STM topograph of Gr/Ir(111). White rounded shapes are buried Ar bubbles. (d) 3D rendering of an 85 nm \times 85 nm STM topograph of Gr/Ir(111) after intercalation of 0.2 ML of Cu. (e) Line profiles along the path define by the two arrows on the 3D rendering of an STM topograph showing one Cu intercalated nanoisland together with Cu intercalated at Ir step edge recorded at $U_t = -0.5$ V (blue line) and $U_t = +1$ V (red line). Parameters are: (c) $U_t = -1$ V, $I_t = 1$ nA, (d) $U_t = -0.5$ V, $I_t = 0.4$ nA.

bias voltage was chosen to obtain a stronger apparent corrugation on Gr/Cu compared to Gr/Ir areas making intercalated areas strikingly visible. Moiré patterns on both areas are observed confirming that graphene covers the entire surface. A graphene overlayer edge can be observed at the center of the image. Next to it, the apparent corrugation is increased. One can therefore conclude that the intercalant can be found at step edges.

The migration of Cu atoms to Gr/Ir step edges can be easily understood in the light of the epitaxial growth of Cu on bare Ir(111) as displayed in Fig. 2. Although Cu growth at room temperature in the submonolayer regime leads to dendritic nanoislands (Fig. 2(a)), all Cu atoms migrate to Ir step edges after annealing at 775 K leaving no island on terraces (Fig. 2(b)). In addition, the resulting surface is smooth with an higher apparent height than Ir. Cu incorporation at step edges persists when covered with graphene pushing away pre existing graphene step edges in the three main crystallographic directions of the moiré pattern leading to their strong reshaping. The migration of the intercalant towards steps suggests a low diffusion barrier on the Ir under the graphene overlayer. This effect has also been observed for other metals under Gr on Ir^{8,9} and can be reasonably explained by the fact that graphene is physisorbed on Ir(111). On the contrary, beneath chemisorbed graphene, the migration of the intercalant towards steps has not yet been observed probably due to a strong pinning of the graphene on the metal hindering metal diffusion as suggested in the case of Gr/Ni/Rh(111) trilayers.⁴ Nevertheless, the presence of Cu intercalated nanoislands on terraces allow to estimate the diffusion barrier of Cu on Ir to be higher when graphene covers the surface.

In addition to intercalant at step edges, intercalated single layer high metal nanoislands are also observed on upper and lower terraces as shown in Fig. 1(d). Their typical lateral sizes are 10 to 15 nm. They are of hexagonal shape with their edges along the same close packed directions as the graphene moiré superstructure. As intercalated areas at step edges, they also exhibit on their surface, the same periodicity as Gr/Ir(111) accompanied with an increased apparent corrugation.

The actual height of these nanoislands cannot be extracted from line profiles of topographic images since the apparent amplitude of the corrugation appears to be strongly bias voltage dependent. It has been shown for graphene on metals and particularly for Gr on Ir that most of apparent corrugation measured by STM is ascribed to local variation of the density of states.¹⁰ Despite STM, AFM gives access to the actual topography, and recent studies revealed a corrugation of about 0.05 nm for Gr on Ir(111).¹¹ One can reasonably expect the same order of magnitude for Gr on Cu since Gr is also weakly bond to Cu.¹² We have recorded line profiles at two bias voltages at a tunneling current of 400 pA along a path that crosses the three kinds of interfaces, namely Gr/Ir, Gr/Cu at step edge, and Gr/Cu on one nanoisland as shown in Fig. 1(e). An apparent corrugation as high as 0.5 nm is observed at a bias voltage of -0.5 V which is five times higher than the one measured on Gr on Ir at the same bias voltage and one order of magnitude higher to the one measured with AFM. At a bias voltage of $+1$ V, the apparent corrugation on Gr/Cu is smaller ranging from 0.1 to 0.3 nm.

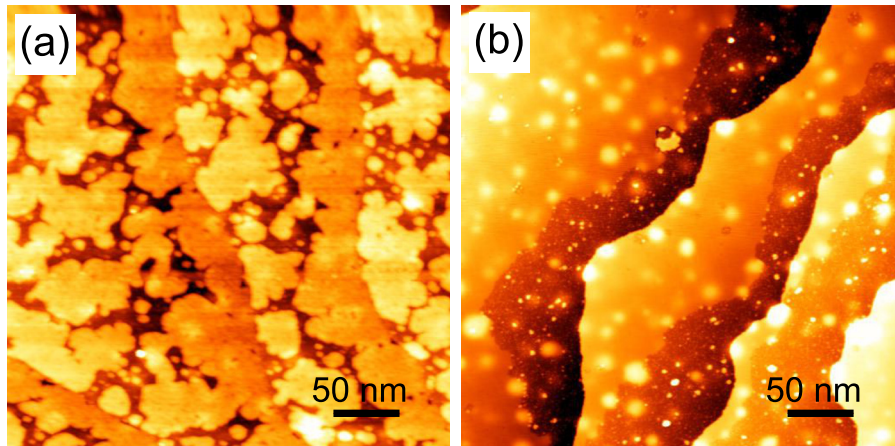


FIG. 2. STM topographs of 0.8 ML Cu/Ir(111) (a) as deposited (b) after annealing up to 775 K for 30 min. Parameters are: (a) and (b) $U_t = -1$ V, $I_t = 1$ nA.

The explanation of this observation requires investigations on the electronic properties and is beyond the scope of the present work. Nonetheless, as mentioned earlier, such effect can be used to highlight intercalated areas in contrast with Gr/Ir areas.

In order to address the growth of Cu beneath the graphene topmost layer, we have recorded STM topographs for increasing amount of intercalant, i.e., 0.12 ML, 0.31 ML, and 0.86 ML as displayed in Figs. 3(a)–3(c), respectively. We have found that for 0.12 ML, an increased apparent surface corrugation is observed next to all step edges as shown in Fig. 3(a). This can be explained by the presence of Cu all along Ir steps beneath the graphene layer. Intercalated Cu nanoislands whose size ranges from 8 to 18 nm are also observed. The corresponding side view of this surface is depicted in Fig. 3(d1), where small amount of Cu

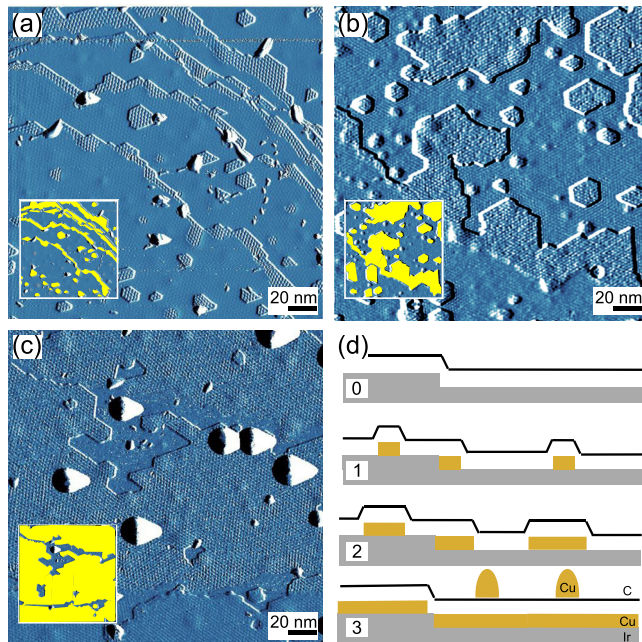


FIG. 3. Constant current STM images of Gr/Ir(111) after Cu intercalation of (a) 0.12 ML, (b) 0.31 ML, and (c) 0.86 ML. Insets are scaled down versions of the large images, where intercalated areas are coloured in yellow. (d) Schematics of the copper intercalation process. Side views of Gr/Ir(111): (0) before intercalation, (1 and 2) upon increasing Cu coverage on Ir, and (3) at coverage close to Cu monolayer completion with Cu left on the topmost graphene layer. Parameters are: (a)–(c) $U_t = -1$ V, $I_t = 1$ nA.

represented both next to Ir step edges and on top of both upper and lower Ir terraces. Upon increasing intercalation coverage to 0.31 ML (Fig. 3(b)), one first observes that the size of the intercalated nanoislands increases accordingly and can be as large as 100 nm as shown on the top of Fig. 3(b). Second, more intercalated material is found next to Ir steps forming flat protuberances and resulting in very indented graphene step edges. These observations can be easily explained if one considers the following scenario depicted in Fig. 3(d2) in the case of Cu adatoms penetrating through the graphene overlayer on a lower terrace of Ir. They can diffuse till they reach either a step edge of a pre-existing intercalated nanoisland on this very lower Ir terrace or a step edge of the upper terrace made either of Cu or Ir. When Cu atoms reach the step edge of the upper terrace, they push away the overlayer resulting in indented graphene step edges. Finally, for 0.86 ML, the overall appearance is a flat surface presenting the high moiré corrugation related to intercalated Cu. Only little less corrugated areas corresponding to Gr on Ir without Cu are left as seen in the center of the STM topograph displayed in Fig. 3(c). Intercalated nanoislands are no longer observed since they merged forming larger intercalated areas as schematically depicted in Fig. 3(d3). The coalescence of Cu areas results in less numerous graphene step edges and therefore in a smoother surface. Note that material that has not been intercalated is still on top of the carbon overlayer forming several nanometers high nanoislands with rounded shape.

In the following paragraphs, we will address the intercalation mechanism. Previous works have shown different paths for intercalation below graphene epitaxially grown on a metal substrate. It seems well established that intercalation can occur via pre existing extended defects in graphene such as wrinkles, domain boundaries or open edges.^{4,13,14} Some recent studies have proposed an alternative path for intercalation via the formation of adatom aided atomic scale defect.¹⁵ In all cases, the intercalation process seems to depend strongly on the initial structural quality of graphene as well as on a subtle balance between the interaction strength of intercalant/carbon and carbon/substrate.

In our case, point defects formation in the graphene topmost layer is unambiguously observed by means of atomically resolved STM topographs recorded after intercalation. A typical example of an intercalated area surrounded

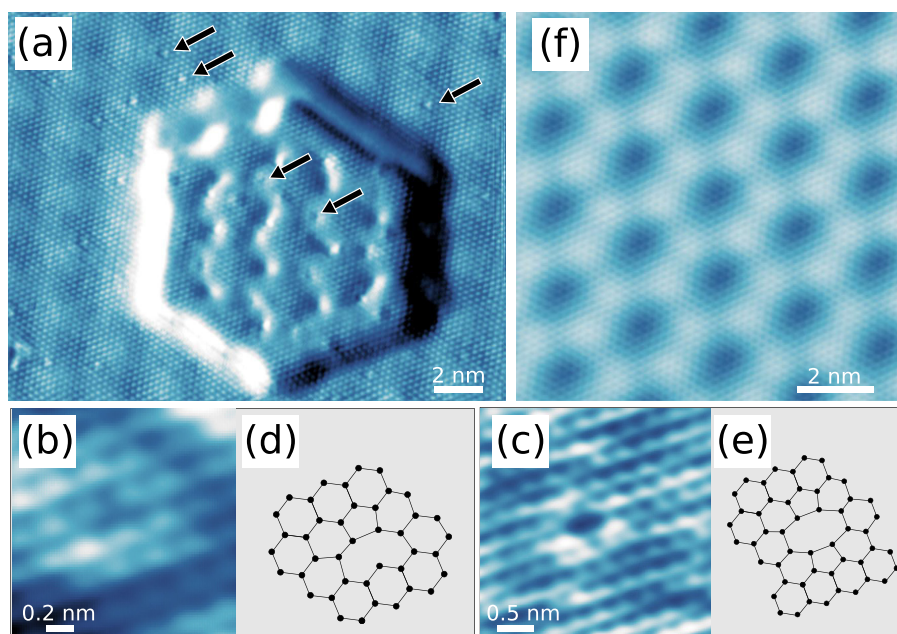


FIG. 4. (a) Constant current STM image of Gr/0.2 ML Cu/Ir(111) showing an intercalated nanoisland. Arrows point to atomic defects both on Gr/Ir and Gr/Cu areas. Zoom in STM topographs centered on carbon mono (b) and di-vacancy (c). Ball and stick models of a reconstructed (d) single, (e) double vacancy in graphene. (f) Atomically resolved STM topograph of Gr/Ir(111) after annealing to 775 K for 1 h. Parameters are: (a) $U_t = 150$ mV, $I_t = 2$ nA, (b) and (c) $U_t = 10$ mV, $I_t = 6$ nA, (d) $U_t = 50$ mV, $I_t = 2$ nA.

by Gr/Ir is displayed in Fig. 4(a). Point defects are pointed by arrows in the figure and are speckled across both on Gr/Ir and Gr/Cu interfaces. It is noteworthy to underline that such atomic defect has never been observed on the Gr/Ir surface before Cu deposition. A comparison between STM topographs at the defects (Figs. 4(b) and 4(c)) and previous theoretical calculations¹⁶ allows us to clearly identify the nature of these defects to be carbon single (Fig. 4(b)) and (5-8-5) divacancy (Fig. 4(c)). As an illustration, ball and sticks models of these two structural defects are displayed in Figs. 4(d) and 4(e).

According to these observations, one can reasonably assume that carbon vacancies have been created by interaction with Cu atoms and offer a possible path through the graphene layer. This assumption is supported by previous works showing that although the energy formation of single and double vacancies in pristine graphene is high (about 7 eV),¹⁷ it can be greatly reduced in the case of metal-supported graphene as shown for Gr/Cu(111)¹⁸ or in the presence of metal adatoms.¹⁹ Moreover, as point defects are still visible after intercalation, one can claim that there is no or little self healing of the carbon layer at 775 K.

Finally, in order to assert that point defect formation was metal aided and to rule out any interaction during annealing with foreign species that could be present in the preparation chamber (such as H_2O , H_2 , O_2 or CO), a Gr/Ir sample was annealed for 1 h at 775 K. As a result, no such point defect in the graphene overlayer was observed as shown by a typical atomically resolved STM topographs of Gr/Ir in Fig. 4(f).

As a conclusion, intercalation of Cu atoms at the graphene/Ir(111) interface has been observed at 775 K. We have shown that the growth of Cu on Ir(111) beneath graphene is pseudomorph. The surface morphology has been described for increasing Cu coverage. The intercalated Cu atoms can diffuse towards step edges leading to a strong reshaping of graphene edges. Monolayer high metal nanoislands of hexagonal shape are also formed on terraces. They increase in size and finally coalesce with increasing Cu coverage. Cu

penetration path was identified to be through of carbon vacancies formed by interaction with Cu atoms. This work illustrates the fact that Cu intercalation is harmful for graphene epitaxially grown on Ir(111). Nevertheless, the back-side of graphene can be used to create nanostructures and thin films with new shape and lattice constant that can result in interesting electronic properties. Finally, Cu intercalation is expected to modify the Dirac cone band structure of graphene by doping or band gap opening.²⁰ Such effects can be measured by ARPES and STS.

We gratefully acknowledge L. Moreau for his technical support on this work and I. Gerber for fruitful discussions.

¹M. S. Dresselhaus and G. Dresselhaus, *Adv. Phys.* **51**, 1 (2002).

²R. R. Meier, J. Sloan, R. E. Dunin-Borkowski, A. I. Kirkland, M. C. Novotny, S. R. Bailey, J. L. Hutchison, and M. L. H. Green, *Science* **289**, 1 (2000).

³Yu. S. Dedkov, M. Fonin, U. Rüdiger, and C. Laubschat, *Appl. Phys. Lett.* **93**, 022509 (2008).

⁴M. Sicot, P. Leicht, A. Zusan, S. Bouvron, O. Zander, M. Weser, Y. S. Dedkov, K. Horn, and M. Fonin, *ACS Nano* **6**, 151 (2012).

⁵A. T. N'Diaye, J. Coraux, T. N. Plasa, C. Busse, and T. Michely, *New J. Phys.* **10**, 043033 (2008).

⁶I. Pletikosić, M. Kralj, P. Pervan, R. Brako, J. Coraux, A. T. N'Diaye, C. Busse, and T. Michely, *Phys. Rev. Lett.* **102**, 056808 (2009).

⁷X. Li, W. Cai, J. An, S. Kim, J. Nah, D. Yang, R. Piner, A. Velamakanni, I. Jung, E. Tutuc *et al.*, *Science* **324**, 1312 (2009).

⁸D. Pacilé, P. Leicht, M. Papagano, P. M. Sheverdyeva, P. Moras, C. Carbone, K. Krausert, L. Zielke, M. Fonin, Y. S. Dedkov *et al.*, *Phys. Rev. B* **87**, 035420 (2013).

⁹R. Decker, J. Brede, N. Atodiresei, V. Caciuc, S. Blügel, and R. Wiesendanger, *Phys. Rev. B* **87**, 041403(R) (2013).

¹⁰E. N. Voloshina, E. Fertitta, A. Garhofer, M. Fonin, A. Thissen, and Yu. S. Dedkov, *Sci. Rep.* **3**, 1072 (2013).

¹¹S. K. Hämalainen, M. P. Boneschanscher, P. H. Jacobse, I. Swart, K. Pussi, W. Moritz, J. ko Lahtinen, P. Liljeroth, and J. Sainio, *Phys. Rev. B* **88**, 201406(R) (2013).

¹²G. Giovannetti, P. Khomyakov, G. Brocks, and V. Karpan, *Phys. Rev. Lett.* **101**, 026803 (2008).

¹³P. Sutter, J. T. Sadowski, and E. A. Sutter, *J. Am. Chem. Soc.* **132**, 8175 (2010).

¹⁴L. Jin, Q. Fu, Y. Yang, and X. Bao, *Surf. Sci.* **617**, 81 (2013).

- ¹⁵L. Huang, Y. Pan, L. Pan, M. Gao, W. Xu, Y. Que, H. Zhou, Y. Wang, S. Du, and H.-J. Gao, *Appl. Phys. Lett.* **99**, 163107 (2011).
- ¹⁶F. Banhart, J. Kotakoski, and A. V. Krasheninnikov, *ACS Nano* **5**, 26 (2011) and references therein.
- ¹⁷A. A. El-Barbary, R. H. Telling, C. P. Ewels, M. I. Heggie, and P. R. Briddon, *Phys. Rev. B* **68**, 144107 (2003).
- ¹⁸L. Wang, X. Zhang, H. L. W. Chan, F. Yan, and F. Ding, *J. Am. Chem. Soc.* **135**, 4476 (2013).
- ¹⁹D. W. Boukhvalov and M. I. Katsnelson, *Appl. Phys. Lett.* **95**, 023109 (2009).
- ²⁰H. Vita, S. Böttcher, K. Horn, E. N. Voloshina, R. E. Ovcharenko, Th. Kampen, A. Thiessen, and Yu. S. Dedkov, *Sci. Rep.* **4**, 1 (2014).